Supporting Information

for

Biaxially Oriented Films of Grafted-Polypropylene with Giant Energy Density and High Efficiency at 125 °C

Junluo Li[1], Shaojie Wang[1], Yujie Zhu[1], Zhen Luo[1], Ya-Ru Zhang[2], Qing Shao[2], Hui Quan[2], Mingti Wang[2], Shixun Hu[1], Mingcong Yang[1], Jing Fu[1], Rui Wang[1], Jun Hu[1], Hao Yuan[2,*], Jinliang He[1,*], Qi Li[1,*]

[1] State Key Laboratory of Power Systems, Department of Electrical Engineering, Tsinghua University, Beijing 100084, China.
E-mail: qili1020@tsinghua.edu.cn
E-mail: hejl@tsinghua.edu.cn

[2] SINOPEC Beijing Research Institute of Chemical Industry, Beijing 100013, People's Republic of China, Beijing 100013, China
E-mail: yuanhao.bjhy@sinopec.com

Table S1 Thermal Properties for BO-(PP-g-MMA) and BOPP.

Sample	Melting temperature (°C)		Melting enthalpy (J/g)		Crystallinity (%)	
	Heating 1	Heating 2	Heating 1	Heating 2	Heating 1	Heating 2
BOPP	168.99	163.84	104.2	91.47	49.86%	43.77%
BO-(PP-g-MMA)-2.5%	169.94	163.1	100.5	88.01	48.09%	42.11%
BO-(PP-g-MMA)-5%	169.74	164.06	102.8	90.29	49.19%	43.20%
BO-(PP-g-MMA)-7.5%	170.27	163.5	98.22	84.28	47.00%	40.33%
BO-(PP-g-MMA)-10%	169.07	164.3	96.52	84.28	46.18%	40.33%

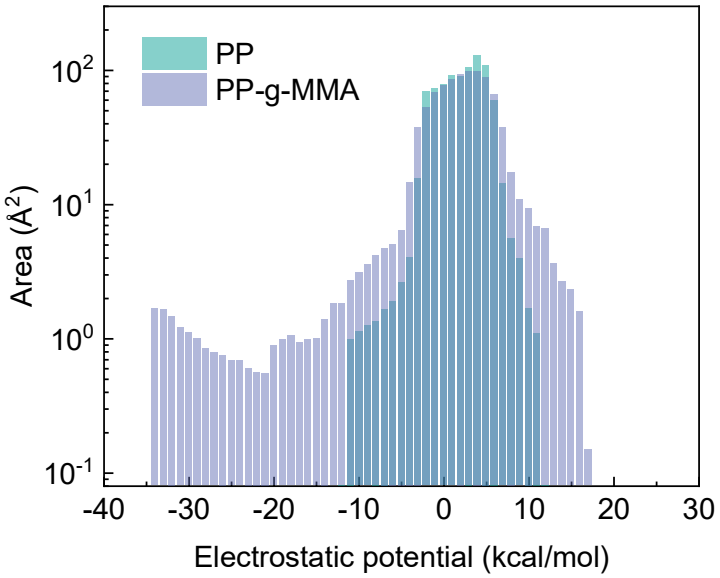

Figure S1 Area percentage of Electrostatic potential of PP and PP-g-MMA

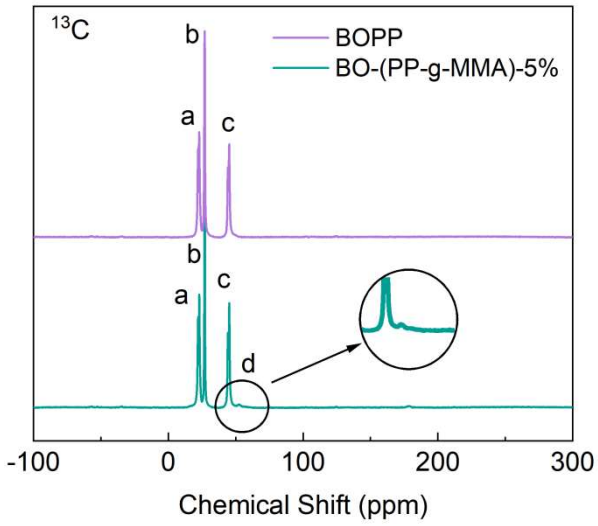

Figure S2 SSNMR spectra of BO-(PP-g-MMA)-5% and BOPP

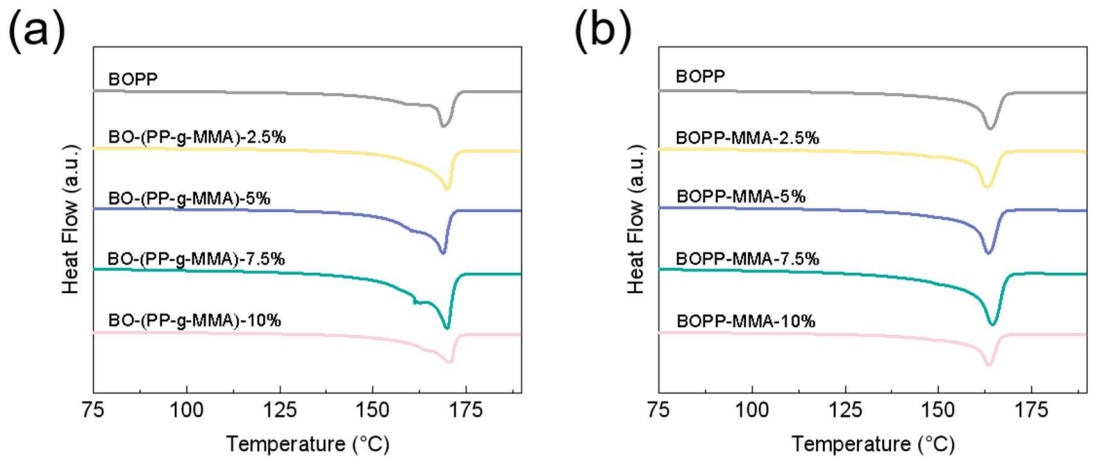

Figure S3 DSC thermograms for BO-(PP-g-MMA) and BOPP. (a) Heating 1 and (b) Heating 2.

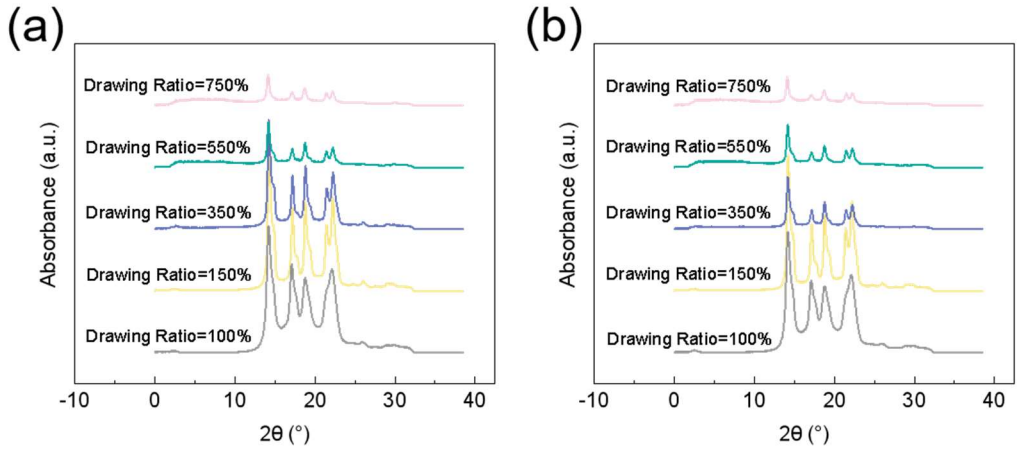

Figure S4 1D integrated WAXD curves of (a) PP-g-MMA-5% and (b) PP.

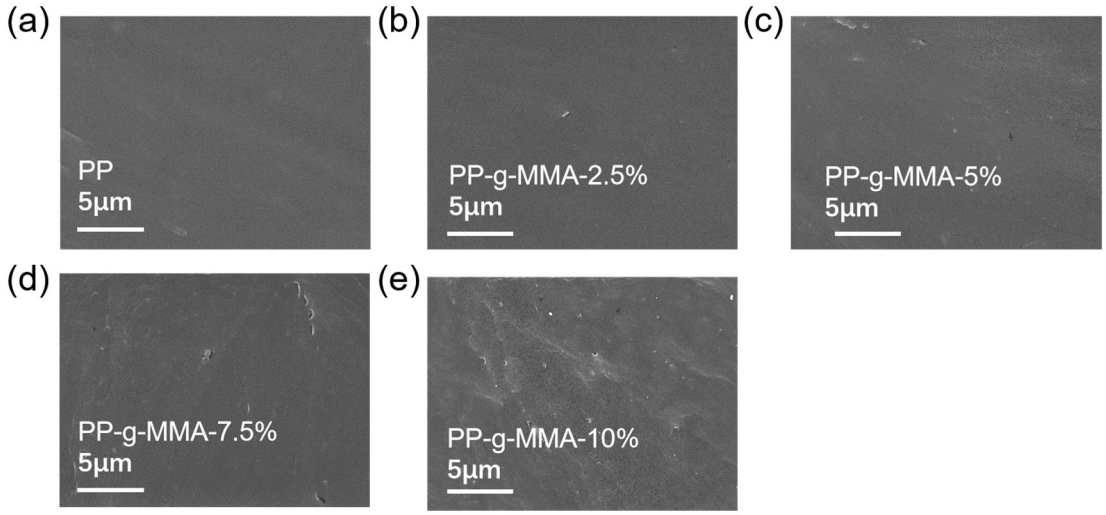

Figure S5 Cross-sectional SEM images of PP and PP-g-MMA. (a) PP, (b) PP-g-MMA-2.5%, (c) PP-g-MMA-5%, (d) PP-g-MMA-7.5% and (e) PP-g-MMA-10%.

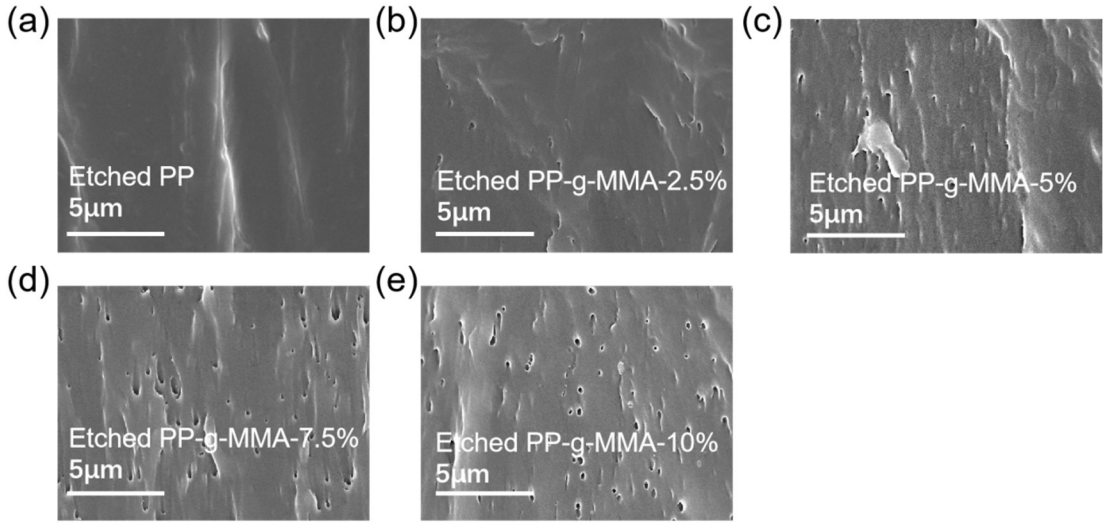

Figure S6 Cross-sectional SEM images of PP and PP-g-MMA after etched by xylene. (a) PP, (b) PP-g-MMA-2.5%, (c) PP-g-MMA-5%, (d) PP-g-MMA-7.5% and (e) PP-g-MMA-10%.

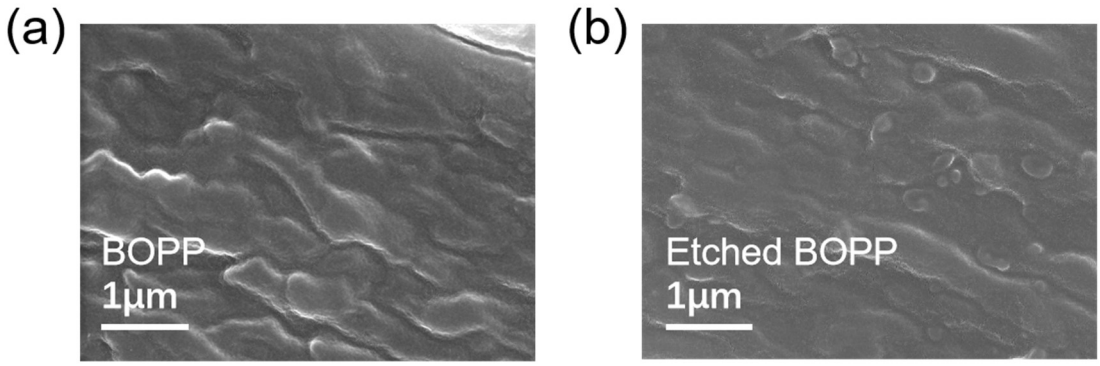

Figure S7 Cross-sectional SEM images of (a) BOPP and (b) Etched BOPP by xylene.

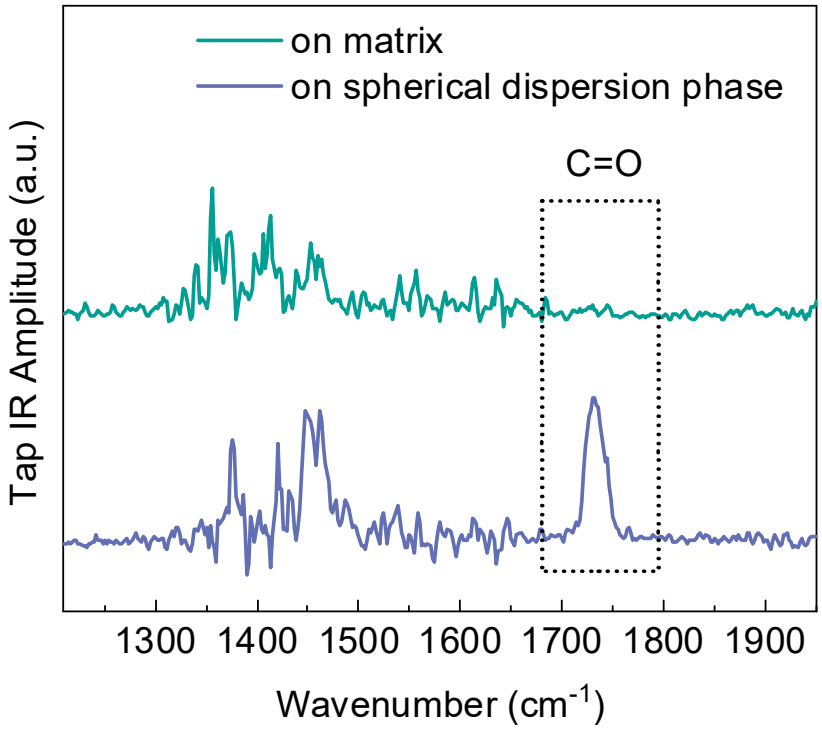

Figure S8 NanoIR spectroscopy spectrum on matrix and spherical dispersion phase for BO-(PP-g-MMA)-5%.

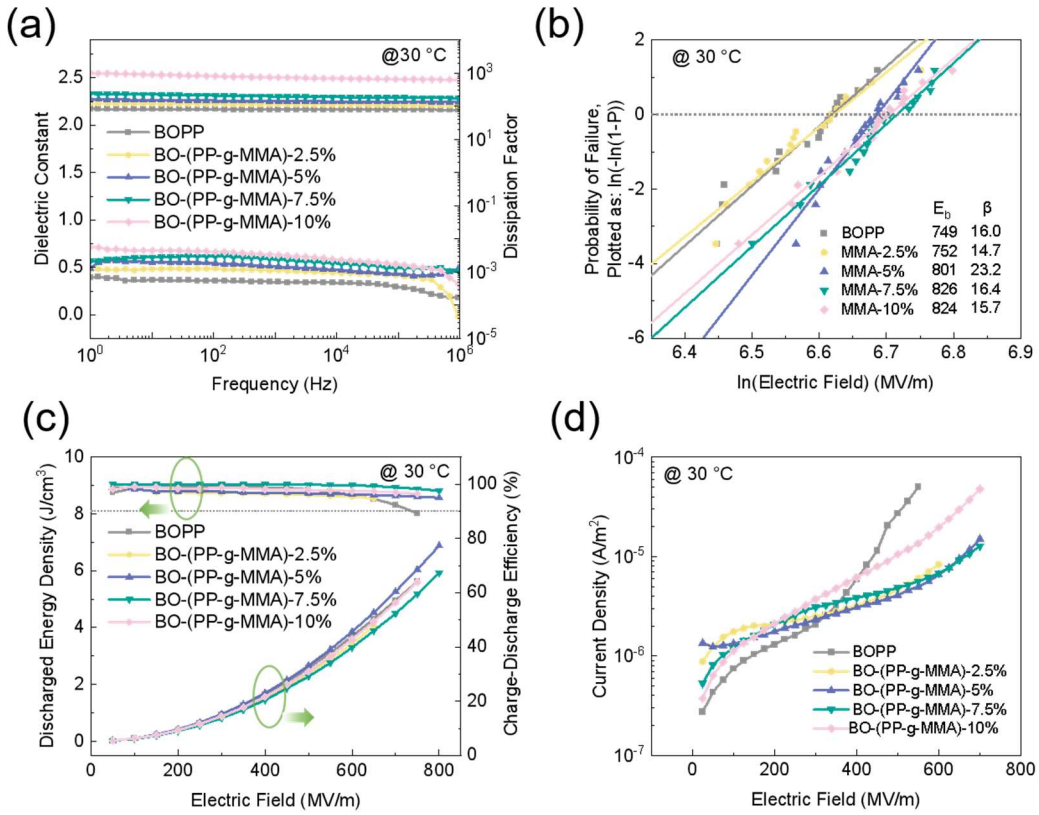

Figure S9 Room-temperature energy storage performance of BO-(PP-g-MMA) and BOPP. (a) Frequency dependent dielectric constant and dissipation factor at 30 °C. (b) Weibull distribution of the breakdown strength at 30 °C. (c) Charge-discharge efficiency and discharged energy density at 30 °C. (d) Leakage current density at 30 °C.

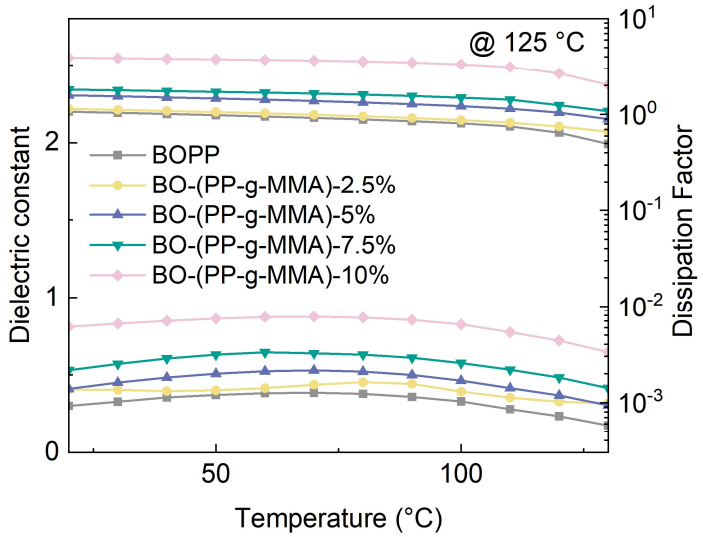

Figure S10 Temperature dependence of the dielectric constant and dissipation factor

of BOPP and grafted BOPP

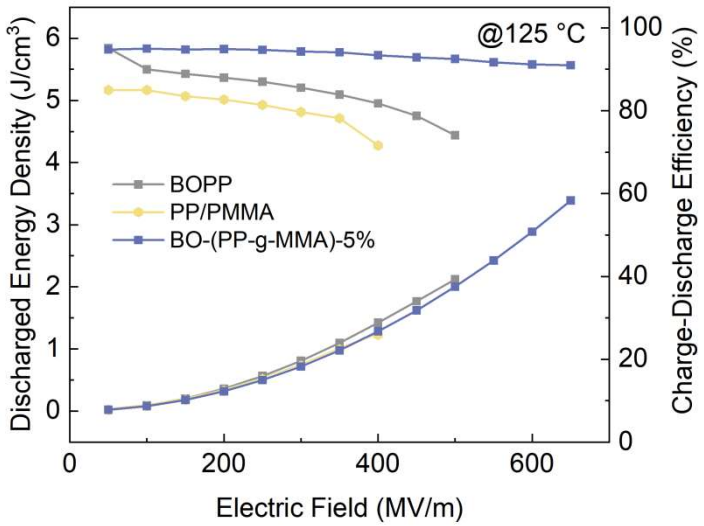

Figure S11 Field-dependent energy density and discharge efficiency of BOPP, PP/PMMA and BO-(PP-g-MMA)-5% at 125 °C.

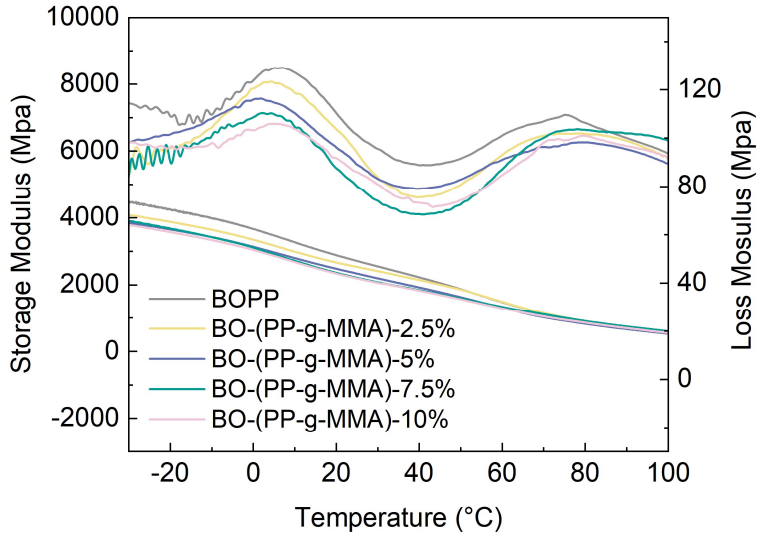

Figure S12 Storage modulus and loss modulus of BOPP and grafted BOPP

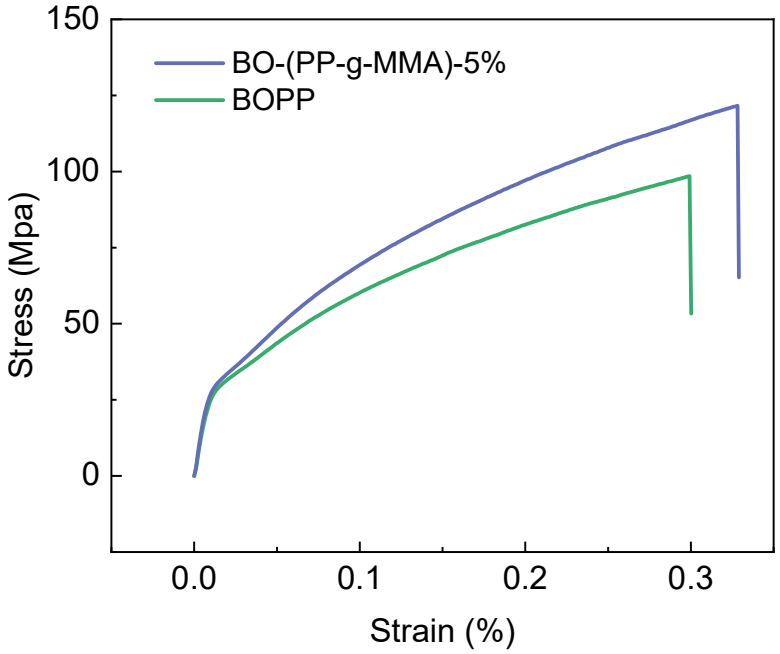

Figure S13 Strain-stress curve of BOPP and BO-(PP-g-MMA)-5%

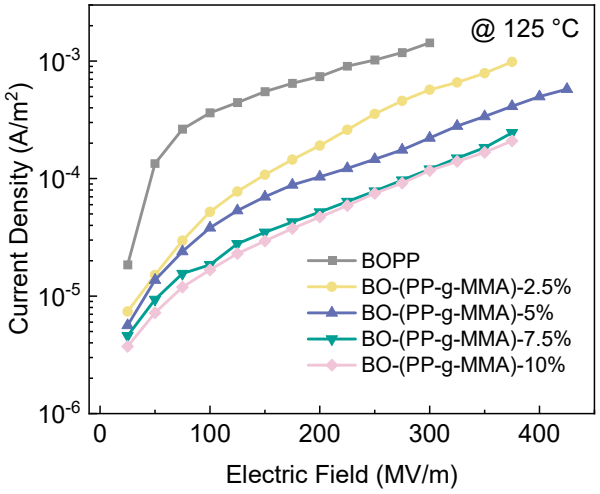

Figure S14 High-temperature leakage current density of BO-(PP-g-MMA) and BOPP.

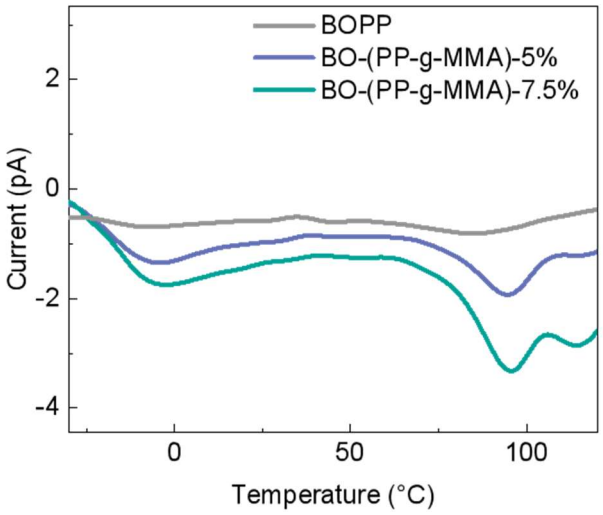

Figure S15 Thermally stimulated current spectra of BO-(PP-g-MMA)-5%, BO-(PP-g-MMA)-7.5% and BOPP under the polarization electric field of 50MV/m.